

**$^{131}\text{Xe}$ , a New NMR Probe of Void Space in Solids<sup>†</sup>**

Igor L. Moudrakovski, Christopher I. Ratcliffe, and John A. Ripmeester\*

Steele Institute for Molecular Sciences  
National Research Council of Canada  
Ottawa, Ontario, Canada K1A 0R6

Received September 28, 2000

Revised Manuscript Received December 12, 2000

Nearly 20 years ago, the  $^{129}\text{Xe}$  ( $I = 1/2$ ) isotope was identified as an NMR probe of void space in solids, with the isotropic chemical shift sensitive to void size, and the anisotropic shift to void symmetry.<sup>1a</sup> Since that time numerous examples of applications have been presented and reviewed,<sup>1b</sup> and considerable progress has been made in the understanding of Xe chemical shifts.<sup>1c</sup> Xenon has a second isotope,  $^{131}\text{Xe}$  ( $I = 3/2$ ) that also has promise as a probe of void space, and since it has a quadrupole moment there is considerable potential for information that is unique and complementary to that obtainable from the spin  $1/2$  isotope.  $^{131}\text{Xe}$  has 21.2% natural abundance, a relatively low resonance frequency (24.6 MHz in a magnetic field of 7.05 T), and a relatively large quadrupole moment<sup>2</sup> of  $-0.12 \times 10^{-24} \text{ cm}^2$ . Its NMR sensitivity is only about 10% of that for  $^{129}\text{Xe}$ . These properties conspire to make the NMR spectroscopy of  $^{131}\text{Xe}$  in solid phases quite challenging.

To date, the NMR applications of  $^{131}\text{Xe}$  mostly include studies in the isotropic liquid phase and anisotropic liquid crystal media, giving information on relaxation due to fluctuating electric field gradients,<sup>3</sup> and the partially averaged quadrupole coupling constants (QCC).<sup>3</sup> Recently, supercritical  $^{131}\text{Xe}$  has been used also as a contrast agent for microimaging of aerogels,<sup>4</sup> and gas phase  $^{131}\text{Xe}$  NMR has been used to investigate macroscopic void space through the small but characteristic residual quadrupolar coupling.<sup>5</sup> In the solid state  $^{131}\text{Xe}$  NMR has been reported only for frozen xenon,<sup>6</sup> where the cubic lattice ensures a zero QCC and the line is very narrow. Without any previous experience in obtaining solid-state spectra of  $^{131}\text{Xe}$ , it is difficult to know what to expect in terms of spectral width and relaxation, as these parameters are entirely a function of the specific lattice sites occupied. With the availability of higher fields it becomes possible to search for the appropriate resonances with some hope of success. In this contribution we show that it is possible to obtain spectra and to extract quadrupole coupling parameters for Xe atoms trapped in well-defined sites in solids. Indications are that these parameters are sensitive to longer-range interactions than the chemical shifts for the spin- $1/2$  isotope. Also, we show that dynamics are probed on an unusually wide time scale, and this should be so for all central transitions of half-integral quadrupolar nuclei. The two xenon isotopes have every prospect of being a powerful and

unique set of complementary NMR probes of both magnetic and electronic environments in the solid state, including dynamics.

$^{129}\text{Xe}$  and  $^{131}\text{Xe}$  NMR spectra were recorded at different magnetic field strengths for a number of solids containing xenon.<sup>7,8</sup> The  $^{131}\text{Xe}$  spectra generally were broad, with a strong field dependence that suggested a large contribution from second-order quadrupole coupling (QC). Especially for the higher fields it was possible to fit<sup>9</sup> the fine structure in terms of a quadrupole coupling constant (QCC),  $\chi$ , and asymmetry parameter,  $\eta$ .

The simplest example is that of xenon/ $\beta$ -quinol clathrate in which there is only one type of Xe site. Each Xe fits tightly in the axially symmetric (3), slightly elongated (prolate) cages<sup>10,11</sup> of the quinol host. This environment is reflected in the details of the chemical shift anisotropy (CSA) powder pattern observed in the  $^{129}\text{Xe}$  spectrum, Figure 1a and Table 1: The large shift corresponds to a small cage, the positive anisotropy to the elongation of the cage and  $\eta = 0$  to the axial symmetry.<sup>11</sup> The  $^{131}\text{Xe}$  spectrum, Figure 1b, shows the central transition ( $1/2 \rightarrow -1/2$ ) powder line shape dominated by a very large QCC of 5.85 MHz. This is the first direct measurement of a  $^{131}\text{Xe}$  QCC of such magnitude and demonstrates that the electric field gradient (EFG) giving rise to the QC is very sensitive to the nonspherical nature of the cage. The asymmetry parameter  $\eta = 0$  again reflects the axial symmetry of the xenon site.

In another organic clathrate, Dianin's compound, the dumbbell-shaped cages can be either singly or doubly occupied, where in the latter instance the two Xe atoms are essentially in van der Waals' contact with each other.<sup>12</sup> In either case, the Xe atoms are situated on a 3-fold axis in the lattice. The two overlapping  $^{131}\text{Xe}$  signals, Figure 1d, show axial anisotropies ( $\eta = 0$ ) and can be assigned by comparing their intensities with those of the  $^{129}\text{Xe}$  signals, Figure 1c. Interestingly, the magnitudes of the Xe chemical shift anisotropies at the two sites do not scale with the QCCs (Table 1), indicating that the second xenon atom causes the magnetic anisotropy to decrease, although the EFG increases in magnitude.

Another relatively straightforward case is that of structure II clathrate hydrates with Xe in the smaller of the two types of cage. With tetrahydrofuran (THF) in the large cage,<sup>13,14</sup> the line shape fit gave an asymmetry parameter of  $\eta = 0.1$ , Table 1, which is

(7)  $^{131}\text{Xe}$  NMR spectra were recorded on Bruker AMX-300, DSX-400, and AMX-600 spectrometers at frequencies of 24.6, 32.8, and 49.2 MHz (magnetic field 7.05, 9.4, and 14.1 T, respectively), using home-built probes with 10 mm solenoid coils. A spin-echo pulse program<sup>8</sup> was used for all static experiments. Static and MAS  $^{129}\text{Xe}$  spectra were acquired at 83.0 MHz (7.05 T) with CP ( $\omega_{\text{IH}} = 40 \text{ kHz}$ , CP time 5 ms, recycle 4 s). All spectra were obtained at ambient temperature and referenced to gaseous Xe extrapolated to 0 pressure (0 ppm). A Xe solution in  $\text{H}_2\text{O}$  was used as a secondary standard. The WinSolids program, kindly supplied by K. Eichele,<sup>9</sup> was used for simulations. CSAs determined from  $^{129}\text{Xe}$  spectra were used as fixed constraints in simulations of the  $^{131}\text{Xe}$  spectra. Xe clathrates of quinol and Dianin's compound were prepared by recrystallizing the solids from ethanol and decanol solutions, respectively, under a few atmospheres of xenon. Clathrate hydrates were prepared by sealing into 10 mm o.d. Pyrex tubes finely powdered ice, the appropriate guest (THF or 1,1,1-dichlorofluoroethane) and sufficient xenon to form the desired material. Samples were annealed for at least a week before recording spectra.

(8) Kunwar, A. C.; Turner, G. L.; Oldfield, E. *J. Magn. Res.* **1986**, *69*, 124.

(9) Eichele, K.; Wu, G.; Wasylishen, R. E.; Britten, J. F. *J. Phys. Chem.* **1995**, *99*, 1030–1037. (b) Eichele, K.; Wasylishen, R. E. *J. Magn. Res. A* **1994**, *106*, 46.

(10) Powell, H. M. In *Non-Stoichiometric Compounds*; Mandelcorn, L., Ed.; Academic Press: New York, 1964.

(11) Ripmeester, J. A.; Ratcliffe, C. I.; Tse, J. S. *J. Chem. Soc., Faraday Trans. 1* **1988**, *84*, 3731.

(12) Lee, F.; Gabe, E.; Tse, J. S.; Ripmeester, J. A. *J. Am. Chem. Soc.* **1988**, *110*, 6014.

(13) Clathrate hydrates are nonstoichiometric; Davidson, D. W. In *Water, a Comprehensive Treatise*; Franks, F., Ed.; Plenum Press: New York, 1975.

(14) Jeffrey, G. A. In *Comprehensive Supramolecular Chemistry*; Atwood, J. L., Davies, J. E. D., MacNicol, D. D., Vogtle, F., Lehn, J.-M., Eds.; Pergamon, Elsevier Science: New York, 1996; Vol. 6, Chapter 23, p 757.

<sup>†</sup> NRCC No.: 43864.

(1) Ripmeester, J. A. *J. Am. Chem. Soc.* **1982**, *104*, 289; Ito, T.; Fraissard, J. *J. Chem. Phys.* **1982**, *76*, 5225. (b) Ratcliffe, C. I. *Ann. Rep. NMR Spectrosc.* **1998**, *36*, 124; Raftery, D.; Chmelka, B. F. *NMR Basic Principles and Prog.* **1994**, *30*, 111. (c) Jameson, C. J.; Jameson, A. K.; Baello, B. I.; Lim, H.-M. *J. Chem. Phys.* **1994**, *100*, 5965; Jameson, C. J.; Jameson, A. K.; Lim, H.-M. *J. Chem. Phys.* **1996**, *104*, 1709.

(2) Raghavan, P. *At. Data Nucl. Data Tables* **1989**, *42*, 189.

(3) In liquid crystals, the electric field gradient (EFG) has a nonzero average value, and the resonance signal is split into 2I components. (a) Jokisaari, J. *Prog. Nucl. Magn. Res. Spectrosc.* **1994**, *26*, 1. (b) Diehl, P.; Jokisaari, J. *J. Magn. Res.* **1990**, *88*, 660. (c) Ylihautala, M.; Ingman, P.; Jokisaari, J.; Diehl, P. *Appl. Spectrosc.* **1996**, *50*, 1435. (d) Saba, G.; Casu, M.; Lai, A. *Int. J. Quantum Chem.* **1996**, *59*, 343.

(4) Pavlovskaya, G.; Blue, A. K.; Gibbs, S. J.; Haake, M.; Cros, F.; Malier, L.; Meersmann, T. *J. Magn. Res.* **1999**, *137*, 258.

(5) Meersmann, T.; Smith, S. A.; Bodenhausen, G. *Phys. Rev. Lett.* **1998**, *80*, 1398.

(6) Cho, G.; Moran, L. B.; Yesinowski, J. P. *Appl. Magn. Res.* **1995**, *8*, 549.

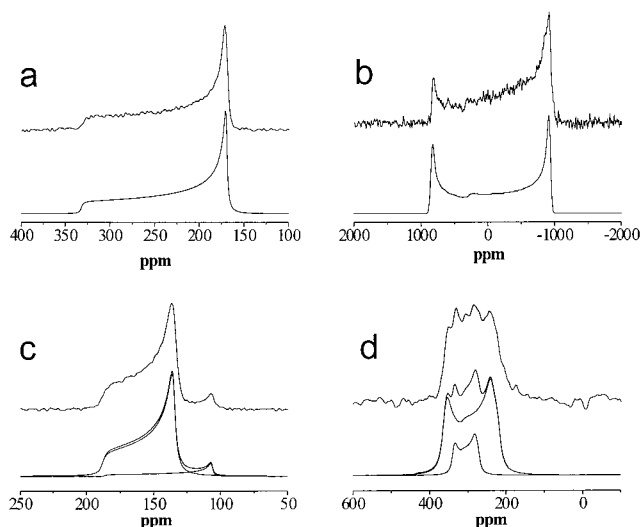


**Figure 1.**  $^{129}\text{Xe}$  (left, at 7.05 T) and  $^{131}\text{Xe}$  (right, at 14.1 T) static solid-state NMR spectra of xenon/ $\beta$ -quinol clathrate (a,b) and xenon/Dianin's compound (c,d), with calculated spectra below each spectrum.

**Table 1.** NMR Parameters of Xe Clathrates

xenonclathrate	details	ave free radius of cage (Å)	chemical shift <sup>a</sup> ( $^{129}\text{Xe}$ )		quadrupole ( $^{131}\text{Xe}$ )	
			$\delta_{\text{iso}}$ ppm ( $\pm 0.2$ )	$\Delta\delta$ ppm ( $\pm 0.5$ )	$\chi$ MHz ( $\pm 0.1$ )	$\eta$ ( $\pm 0.05$ )
quinol	single cage type	$\sim 2.4$	222.1	107.9	5.85	0.0
Dianin's compound	1 Xe/cage	$\sim 3.1^b$	132.6	53.0	1.16	0.0
	2 Xe/cage		151.9	35.1	1.70	0.0
structure II hydrate	THF in large cage	$\sim 2.5$	234.2	-16.6	1.92	0.1
	DCFE in large cage		231.8	-15.7	1.81	0.1
structure I Xe hydrate	small cage	$\sim 2.5$	244.6	0.0	1.33 <sup>c</sup>	$\sim 0.0$
	large cage	$\sim 2.93$	154.9	-19.2	2.52	$\sim 0.1$

<sup>a</sup>  $|\delta_{33} - \delta_{\text{iso}}| > |\delta_{22} - \delta_{\text{iso}}|, |\delta_{11} - \delta_{\text{iso}}|$ ;  $\Delta\delta = \delta_{33} - \delta_{\text{iso}}$ ;  $\eta = |\delta_{22} - \delta_{11}|/|\delta_{33} - \delta_{\text{iso}}|$ ;  $\eta = 0$  for all  $^{129}\text{Xe}$  spectra, within error. <sup>b</sup> Free radius at widest point <sup>c</sup> From fit to second-order shifts at three fields, assuming  $\eta=0$ .

somewhat surprising, as the point group symmetry of the small cage is  $3m$ , requiring the Xe atom to lie on a symmetry axis ( $\eta = 0$  expected). This must indicate that the average local symmetry is less than axial. As indicated below, this should be ascribed to the presence of vacant guest sites.<sup>13</sup> Since the CSA tensor has axial symmetry, it is clear that the QCC tensor probes interactions beyond the cage walls. Similar but distinct spectral parameters were observed for structure II hydrate with 1,1,1 dichlorofluoroethane (DCFE) as the large cage guest, Table 1.

A final case is that of structure I xenon hydrate, where Xe is situated in two cages of different point group symmetry,  $m3$  for the small pentagonal dodecahedral cage, and  $42m$  for the large tetrakaidecahedral cage.<sup>13,14</sup> One remarkable feature of the spectra, well illustrated in Figure 2, is that even though the small cage is a tetrahedral site and does not show fine structure, there is a clear indication of a field-dependent second-order quadrupolar shift that fits a QCC of  $\sim 1.33$  MHz. This can be explained by the presence of the  $^1\text{H}$  disorder in the hydrate lattice, arising from the fact that a proton can be fixed at one of two positions within each H bond, much the same as for ice *Ih* itself. Spatial averaging of  $1/2$ -H's over these positions gives rise to the high crystallographic symmetry. This disorder is static on an NMR time scale at low temperatures, but becomes dynamic as temperature increases until eventually it is sufficiently rapid to affect a number of the NMR parameters. The guest resonance monitors the local symmetry of each cage as follows. The observed QCC can be approximated

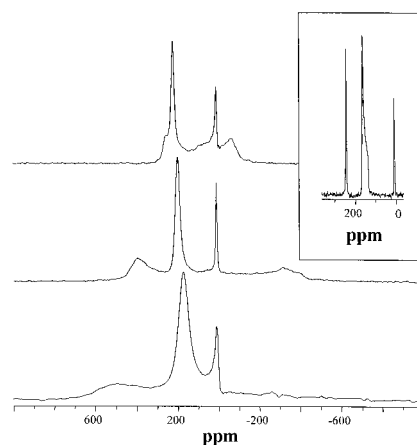


**Figure 2.**  $^{131}\text{Xe}$  static solid-state NMR spectra of structure I xenon hydrate as a function of magnetic field strength (from top: 14.1, 9.4, 7.05 T). Note the obvious shift and broadening of the "pseudo-isotropic" small cage line. The sharp line close to zero shift is from Xe gas. The inset shows the  $^{129}\text{Xe}$  NMR spectrum (7.05 T) on the same scale.

as  $\text{QCC} = \text{QCC}_{\text{ss}} + \text{QCC}_{\text{d}}$ , where the first term comes from site symmetry as determined by the crystal lattice and fixed defects and the second term is due to the  $^1\text{H}$  disorder, and thus it is affected by water molecule dynamics. We note that the fine structure due to  $\text{QCC}_{\text{d}}$  in the central transition is averaged by motions with rates that are of the order of the fine structure splitting  $\sim dQ \sim 10$ 's of kHz. However, these relatively slow motions cause averaging to give a featureless pseudo-isotropic line which still is affected by the second-order shift. Averaging to the true isotropic chemical shift value only takes place when the motions are isotropic and achieve a rate faster than the first-order quadrupolar splittings, thus the order of at least several MHz. Clearly, this complex dependence on dynamics can be very informative but also confusing, as it is easy to interpret the featureless pseudo-isotropic resonance as being at its true isotropic position.

Since cage occupancies are known for Xe structure I hydrate,<sup>16</sup> where the small cages are only 71.6% filled and the large cages 98.1%, it is possible to estimate the number of Xe whose local symmetry will be affected by vacancies. Each large cage is connected, by shared faces, to 4 small and 10 large cages. Each small cage connects to 12 large cages only. The use of simple statistics then leads to the conclusion that  $\sim 78\%$  of all the large cages will have at least one vacant neighboring cage and thus experience a departure from the axial symmetry expected from the symmetrized crystal structure. Once again the EFG is apparently more sensitive to this than the CSA (the  $^{131}\text{Xe}$  NMR spectrum has  $\eta \approx 0.1$ , Table 1). Likewise  $\sim 21\%$  of the small cages should experience a departure from the expected tetrahedral symmetry. Only  $\sim 4\%$  of the total Xe content will occupy these distorted small cages, and thus their minimal contribution to the line shape is not discernible.

In conclusion, we report the first anisotropic solid state  $^{131}\text{Xe}$  NMR spectra and determine a number of quadrupole coupling parameters for trapped xenon. These suggest that  $^{131}\text{Xe}$  NMR is a sensitive probe of the symmetry and dynamics of the local environment, but over a longer-length scale than the CSA. The study of other closed and open systems is underway in our laboratory, and continuing work in this area will ensure the development of applications of the  $^{131}\text{Xe}$  NMR probe also to the void space in zeolites and other porous materials.

JA0035248

(15) Resolved fine structure may, in fact, never be observable, as the disordered water molecules give rise to numerous distinct cage configurations, each with its own set of quadrupole coupling parameters.

(16) Davidson, D. W.; Handa, Y. P.; Ripmeester, J. A. *J. Phys. Chem.* **1986**, *90*, 6549.